JOURNAL OF SOLID STATE CHEMISTRY **127,** 25–30 (1996)
ARTICLE NO. 0352

Crystal Structure and Magnetic Properties of the One-Dimensional Oxide, Sr_3ZnIrO_6: Zinc in Trigonal Prismatic Coordination

Christina Lampe-Önnerud,* Manfred Sigrist,† and Hans-Conrad zur Loye*,[1]

*Department of Chemistry and †Department of Physics, Massachusetts Institute of Technology, Cambridge, Massachusetts 02139

Received March 14, 1996; in revised form July 30, 1996; accepted August 1, 1996

The structure of Sr_3ZnIrO_6 was determined by powder X-ray Rietveld refinement in space group R $\bar{3}$ c (No. 167), a = 9.6392(1) and c = 11.2145(2) Å. Neutron diffraction refinements confirm the structure analysis. The structure contains zinc in a highly unusual trigonal prismatic coordination environment. The structure consists of infinite one-dimensional chains of alternating face-shared IrO_6 octahedra and ZnO_6 trigonal prisms. Magnetic measurements show that Sr_3ZnIrO_6 correlates antiferromagnetically near 20 K. No magnetic ordering, however, was found by the neutron diffraction experiments performed at room temperature and at 10 K. The magnetic data were fit using an Ising model, which gave a coupling value $J/k_B \sim 18.5$.

INTRODUCTION

Low-dimensional materials, both one- and two-dimensional, have long been of interest to chemists and physicists; in particular, the relationship between the crystal structure and the magnetic behavior has been studied (1–3). We have investigated both one- and two-dimensional oxides and have studied their structures and magnetic properties. Two dimensional structures, such as $InFeO_3$ or $InMnO_3$, have exhibited complex field dependent antiferromagnetic interactions (4–6) while one-dimensional oxides, such as Sr_3NiIrO_6, and $Sr_3NiPt_{1-x}Ir_xO_6$, have exhibited combinations of antiferro- and ferromagnetic interactions (7, 8). The discovery of a new class of magnetic behavior, random quantum spin chain paramagnetism (9), has been observed for the first time in the structurally related one-dimensional compound $Sr_3CuPt_{1-x}Ir_xO_6$ (10). This large family of one-dimensional oxides permits a rich substitutional chemistry and we have recently reported the synthesis and structure of a new zinc containing strontium platinum oxide, Sr_3ZnPtO_6 (11). Here we present the synthesis, structure, and magnetic characterizations of the isostructural Sr_3ZnIrO_6, containing zinc in a highly unusual trigonal prismatic oxygen coordination.

EXPERIMENTAL

Sr_3ZnIrO_6 was synthesized via a solid state route using $SrCO_3$ (Alfa, 99.99%), ZnO (Alfa, 99.99%), and Ir metal grains (Engelhard, 99.99%) in a platinum crucible. Stoichiometric quantities were ground and initially calcined at 1073 K for 10 h followed by three heat treatments at 1273 K for 3 days each, with intermittent grindings. Intermediate phase analysis by powder X-ray diffraction showed strontium containing impurity phases due to small evaporative losses of zinc. Therefore, excess ZnO (20 mol%) was added to the sample. Two heat treatments followed at 1273 and 1573 K for 2 days and 20 h, respectively. The dark gray powder sample (5 g) used in this study contained two phases, Sr_3ZnIrO_6, described below, and a small amount of unreacted ZnO (12). Powder X-ray diffraction was performed at 295 K using a Siemens D5000 diffractometer using CuK_α radiation (graphite monochromator). The step-scan covered the range 2.00°–118.01° in steps of 0.03° in 2θ. Three step-scans were collected and summed. For the neutron analysis, a second sample (25 g) was made containing excess ZnO as described above. Neutron diffraction data, collected at the Swedish Research Reactor R2 in Studsvik, included both room temperature and 10 K experiments (steps of 0.08° in the 2θ range of 0.2°–128.04°).

Magnetic measurements of Sr_3ZnIrO_6 were performed on a Quantum Design MPMS SQUID magnetometer. The sample was cooled in zero field before any magnetic data were collected in an applied field of 5 kG over the temperature range 5–300 K. The magnetic data were corrected for the Kel-F sample holder and the presence of the diamagnetic zinc oxide phase.

[1] To whom all correspondence should be addressed.

0022-4596/96 $18.00

TABLE 1
Results from X-Ray (XRD) and Neutron (ND) Rietveld Refinements of Sr_3ZnIrO_6 ($R\bar{3}c$)

Data Cell (Å)	Atom		x	y	z	U_{ISO}	Agreement
XRD, 295 K	Sr	(18*e*)	0.3640(1)	0	$\frac{1}{4}$	0.0102(3)	Rp = 6.63%
a = 9.6392(1)	Zn	(6*a*)	0	0	$\frac{1}{4}$	0.0165(7)	Rwp = 9.07%
b = 11.2145(2)	Ir	(6*b*)	0	0	0	0.0070(3)	Chi^2 = 2.34
	O	(36*f*)	0.1758(5)	0.0241(5)	0.1149(4)	0.007(1)	
ND, 295 K	Sr	(18*e*)	0.3629(2)	0	$\frac{1}{4}$	0.052(6)	Rp = 5.84%
a = 9.6426(8)	Zn	(6*a*)	0	0	$\frac{1}{4}$	0.05(1)	Rwp = 8.87%
b = 11.2093(1)	Ir	(6*b*)	0	0	0	0.031(7)	Chi^2 = 2.11
	O	(36*f*)	0.1729(2)	0.0207(2)	0.1122(2)	0.076(6)	
ND, 10 K	Sr	(18*e*)	0.3640(3)	0	$\frac{1}{4}$	0.028(5)[a]	Rp = 6.09%
a = 9.616(1)	Zn	(6*a*)	0	0	$\frac{1}{4}$	0.028(5)[a]	Rwp = 8.46%
b = 11.183(1)	Ir	(6*b*)	0	0	0	0.028(5)[a]	Chi^2 = 2.42
	O	(36*f*)	0.1741(3)	0.0213(5)	0.1126(2)	0.028(5)[a]	

[a] Overall thermal displacement refined at 10 K.

RESULTS AND DISCUSSION

Structure Refinement

For the refinements of the Sr_3ZnIrO_6 crystal structure, the Rietveld method (13), implemented in the computer program GSAS (14), was used. The structure of Sr_3ZnPtO_6 (11) was used as the starting model. The background was described by refining six coefficients in a shifted Chebyshev polynomial function. Two parameters were used to refine the unit cell and one parameter was included to refine the zero point in 2θ. In order to describe the reflection peak shapes, a pseudo-Voigt function (15) was applied. This function allows the peak profile to vary depending on strain and particle size broadening. In addition, variables accounting for peak asymmetry and a physical shift from the diffractometer axis together with the Gaussian half-width parameters U, V, and W were refined. A preferred orientation correction was also applied. The refinement of the Sr_3ZnIrO_6 crystallographic structure included positional coordinates of strontium and oxygen, and isotropic thermal displacement factors for each atomic position. Since a trigonal prismatic coordination for zinc is rather unusual, attempts were made to refine mixed occupancies in the structure by placing iridium atoms on the zinc positions and vice versa to confirm the accuracy of the model. Similarly, random site substitution between zinc and strontium was tested. No significant (<1%) site mixing was found for either case. The wurtzite structure of ZnO is known (16) and the ZnO phase was included as such in the refinement. Phase fraction refinement showed that the excess of ZnO in the final powder sample was 2.53 wt% for the X-ray sample and 0.75% for the neutron sample. The atomic positions and the final agreement factors for all three refinements are listed in Table 1 and select bond distances are given in Table 2. The observed intensities, the calculated patterns, and their differences are shown in Figs. 1 and 2. The structure of Sr_3ZnIrO_6 consists of one-dimensional infinite chains containing alternating face-sharing slightly distorted IrO_6 octahedra and ZnO_6 trigonal prisms (Fig. 3). Each chain is surrounded by six parallel neighboring chains that are separated by the strontium cations, which are in a distorted square antiprismatic coordination. Within each chain, zinc and iridium are collinearly aligned.

The occurrence of zinc in trigonal prismatic coordination is notable in this structure, since the common coordination environment for zinc in oxides, as well as in most other materials, is tetrahedral (17). While there are some examples of zinc in six-fold, octahedral coordination, such as in $Zn(NH_3)_6^{+2}$ (18), there are few examples of zinc in trigonal prismatic coordination in the literature (11). This makes Sr_3ZnIrO_6 a rare example of a compound with zinc in trigonal prismatic coordination.

Another notable feature of the Sr_3ZnIrO_6 structure is

TABLE 2
Selected Bond Distances from X-Ray (XRD) and Neutron (ND) Refinements of Sr_3ZnIrO_6

Atoms	Bond distances (Å)		
	XRD, 295 K	ND, 295 K	ND, 10 K
Zn–Sr	3.508(1), 3.5994(4)	3.499(2), 3.6036(8)	3.500(3), 3.590(1)
Zn–Ir	2.80363(5)	2.8023(2)	2.7957(3)
Sr–Ir	3.2149(4)	3.2200(9)	3.207(1)
Zn–O	2.197(4)	2.207(2)	2.206(3)
Ir–O	2.047(4)	2.017(2)	2.022(2)
Sr–O	2.462(4), 2.619(5)	2.479(3), 2.642(2)	2.472(3), 2.632(3)
	2.676(4), 2.757(5)	2.659(2), 2.735(3)	2.648(3), 2.724(4)

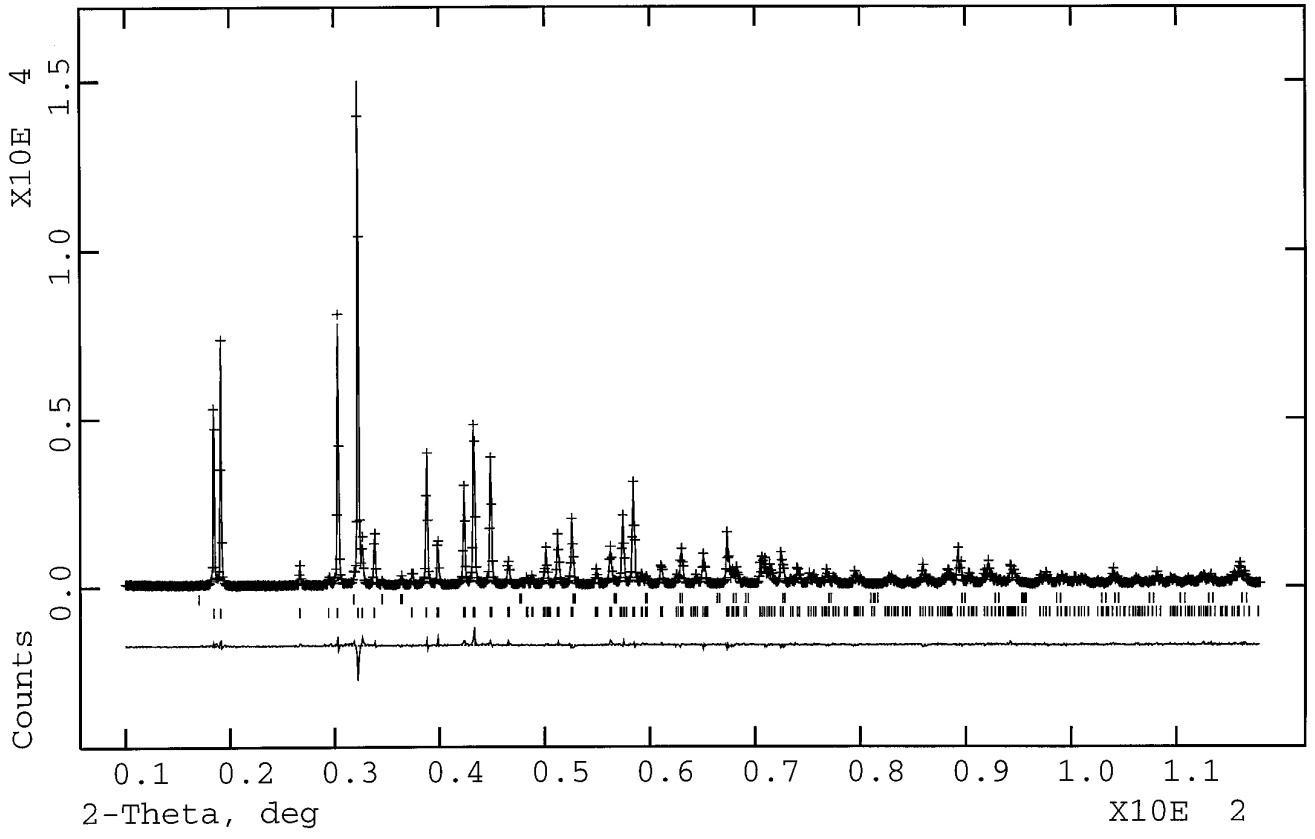

FIG. 1. Observed (dotted) and calculated (solid line) X-ray profile. Tic-marks below the diffractogram represent Sr_3ZnIrO_6 (bottom) and ZnO (top), respectively. The difference line, observed minus calculated, is located at the bottom of the figure.

the presence of face-shared octahedra and trigonal prisms and the resulting short Zn–Ir separation (Zn–Ir = 2.80363(5) Å obtained by X-ray diffraction). There exist a finite number of structures containing infinite chains of face-sharing polyhedra, such as $BaNiO_3$ (19) which contains infinite chains of all face-shared octahedra and Sr_3NiPtO_6 which contains chains of alternating face-shared octahedra and trigonal prisms. One feature of oxides containing face-shared polyhedra is the presence of short metal–metal distances which, however, cannot necessarily be equated with metal–metal bonding. For example, the short Ni–Ni distance of 2.41 Å in $BaNiO_3$ does not result in the formation of nickel–nickel bonds and the material is not metallic (19). Similarly in Sr_3NiPtO_6, which is isostructural with Sr_3ZnIrO_6, the short Ni–Pt distance of 2.799(4) Å was shown by extended Hückel calculations not to result in any direct or indirect metal–metal interactions (20). Consequently, Sr_3ZnIrO_6 is not expected to contain any Zn–Ir bonds and, consistent with this assumption are conductivity measurements which indicate that Sr_3ZnIrO_6 is an insulator.

Magnetism

The magnetic properties of Sr_3ZnIrO_6 arise from the magnetic moments on the Ir ions. Ir(IV) in a slightly distorted octahedral coordination has one unpaired electron, which yields a spin $S = \frac{1}{2}$ degree of freedom. The Curie constant calculated from the susceptibility data (Fig. 4) above 60 K is 0.3236 and corresponds to a magnetic moment of 1.61 μ_B. This compares well with other Ir(IV) containing oxides, such as La_2MgIrO_6 and La_2ZnIrO_6 (21, 22) with effective magnetic moments of μ_{eff} =1.42 μ_B and 1.67 μ_B, respectively. The maximum of the susceptibility at 20 K and the decrease for lower temperatures indicates antiferromagnetic coupling between the Ir spins. The exchange among them occurs mainly along the path of hybridized Ir($5d$)–O($2p$)–Zn($3d$)–O($2p$)–Ir($5d$) orbitals, which yield comparatively weak coupling on the order of 20 K.

In many cases a simple spin model can help in understanding the magnetic properties of such systems and can provide a good fit for the susceptibility data. We may view Sr_3ZnIrO_6 magnetically as a one-dimensional spin $S = \frac{1}{2}$

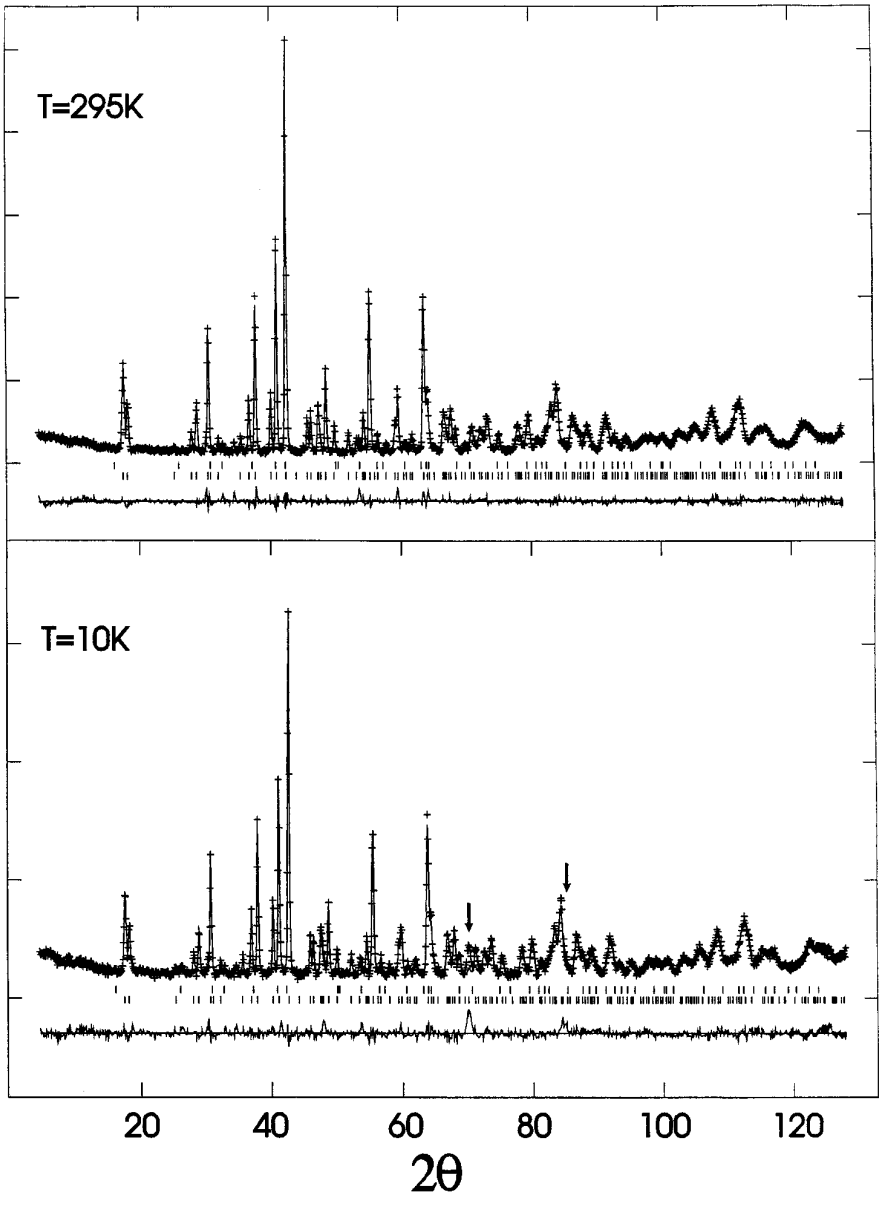

FIG. 2. Observed (dotted) and calculated (solid line) neutron profile at 295 K and 10 K. Tic-marks below the diffractogram represent Sr_3ZnIrO_6 (bottom) and ZnO (top), respectively. The difference line, observed minus calculated, is located at the bottom of each data set. The arrows on the 10 K data set indicate reflections from the cryostat used to cool the sample.

system with nearest neighbor antiferromagnetic interactions. As an example, the $S = \frac{1}{2}$ Heisenberg spin chain with isotropic interaction gives a very convincing fit for the susceptibility of the structurally related compound Sr_3CuPtO_6 (8). However, it does not give an acceptable fit in the present case, where the relatively sharp drop of the susceptibility below the maximum can be attributed to the presence of a gap for the magnetic excitations; the isotropic Heisenberg model does not have such a gap. A typical example of a system with a gap is the spin-Peierls system (alternating Heisenberg model) where in connection with a lattice distortion (doubling of the unit cell) spin singlet dimerization occurs. Such a model gives indeed a reasonable fit to our data (7). However, neither X-ray nor neutron scattering data show any sign of such a structural modification at any temperature. An alternative model is a regular spin chain with anisotropic spin–spin interaction (different coupling strengths for the three spin components, i.e., the *XYZ* model). In particular, the Ising limit, where only the z component of the spins couple, is well-known to have an excitation gap. Such anisotropy can result from spin–orbit coupling which removes, at least partially, the spin rotation

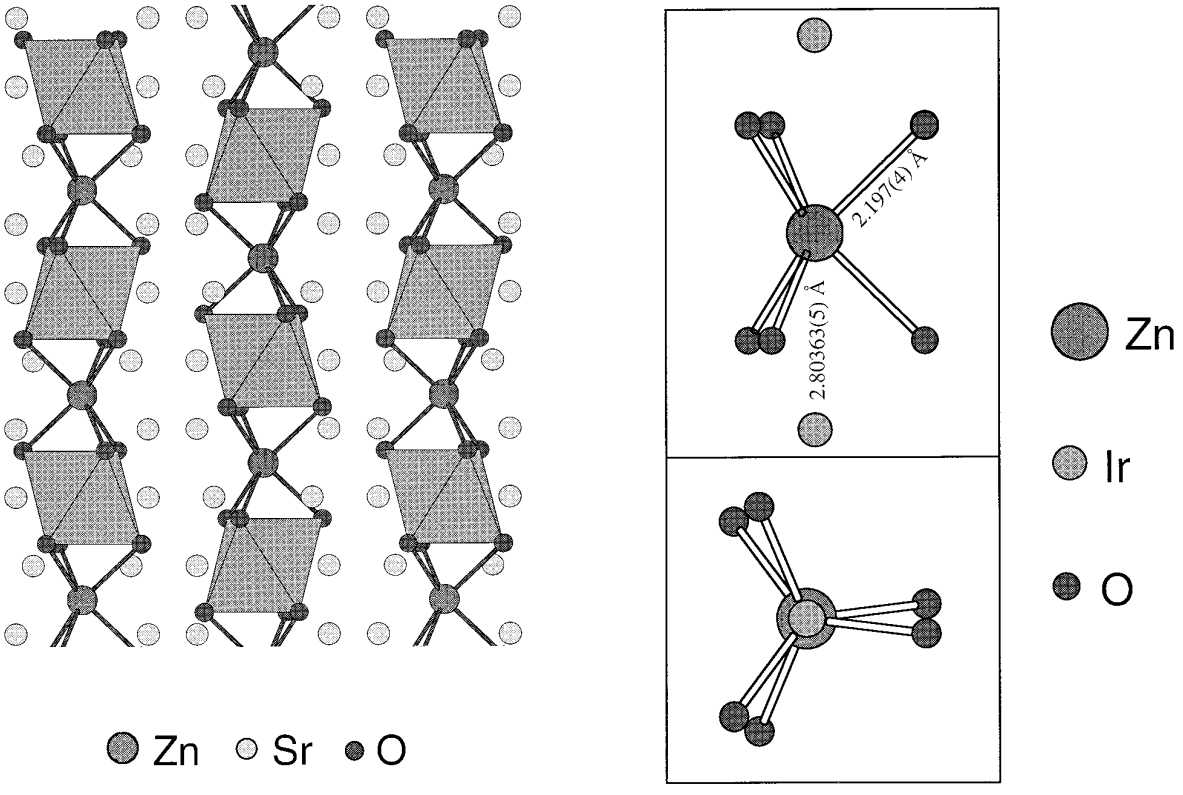

FIG. 3. The one-dimensional chain structure of Sr_3ZnIrO_6 viewed along the *a*-axis is shown on the left. The IrO_6 octahedra are shown as polyhedra, while all other atoms are shown in ball and stick format. The coordination environment around the trigonal prismatically coordinated zinc is shown on the right. Atomic sizes are scaled according to thermal parameters.

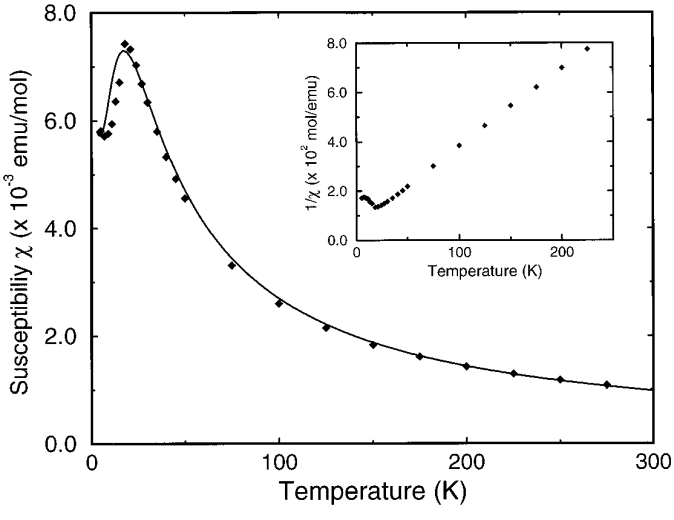

FIG. 4. Magnetic susceptibility plot for Sr_3ZnIrO_6 showing antiferromagnetic ordering with a Neel temperature of 18 K. The inverse susceptibility is shown in the insert. The measured Curie constant is 0.3236 and the corresponding magnetic moment is 1.61 μ_B. The susceptibility data were fit to a one-dimensional Ising model (solid line) with $J/k_B \sim 18.5$.

symmetry. We found that the standard Ising model (23) with a coupling of $J/k_B = 18.5$ K gives a much better fit of the experimental data (Fig. 4) than the isotropic Heisenberg model (24).

The increase of the susceptibility below 10 K can be attributed to a Curie-like (C/T) contribution of uncorrelated spin degrees of freedom. Among other sources such spins can appear in our samples, because the spin chains have a finite length. For chains containing an odd number of $S = \frac{1}{2}$ spin, the ground state is a spin doublet, while an even number of spins does not yield residual spin degrees of freedom. These residual spins couple only very weakly and behave essentially as independent degrees of freedom under thermal fluctuations. A rough estimate based on our fit to the susceptibility gives a residual spin concentration of 0.5%, which can be interpreted as resulting from spin chains of about 200–300 spins. This corresponds to a length of order 0.2 μm which is a reasonable size of the crystallites in our powder samples.

In summary, we have synthesized and characterized the structure and magnetic properties of Sr_3ZnIrO_6, a new oxide containing infinite chains of alternating face-shared IrO_6 octahedra and unusual ZnO_6 trigonal prisms. The

magnetic susceptibility data of this one-dimensional spin $\frac{1}{2}$ system can be fitted to a standard Ising model when the angular average of the susceptibility is taken into account.

ACKNOWLEDGMENTS

We thank James White for his help with the synthesis. The neutron data experiments were made in kind collaboration with Dr. Roland Tellgren and Mr. Håkan Rundlöf at the Swedish Neutron Research Reactor in Studsvik, and are hereby gratefully acknowledged. This work was supported by the Massachusetts Institute of Technology Science Partnership Fund and the Center for Materials Science and Engineering under Grant DMR:9400334. M.S. is grateful for support by the Swiss National Fonds (No. 8220-037229). The purchase of the Siemens D-5000 diffractometer was made possible by an equipment grant from the NSF, CTS-9411901.

REFERENCES

1. R. L. Carlin, ''Magnetochemistry.'' Springer-Verlag, Berlin, 1986.
2. L. J. de Jongh and A. R. Miedema, *Adv. Phys.* **23,** 1 (1974).
3. J. Rouxel, *in* ''Physics and chemistry of materials with Low-Dimensional Structures'' (J. Rouxel, Ed.), Vol. 2. Reidel Publishing, Boston, 1986.
4. J. E. Greedan, M. Bieringer, J. F. Britten, D. M. Giaquinta, and H.-C. zur Loye, *J. Solid State Chem.* **116,** 118 (1995).
5. D. M. Giaquinta, W. M. Davis, and H.-C. zur Loye, *Acta Crystallogr. C* **50,** 5 (1994).
6. D. M. Giaquinta and H.-C. zur Loye, *J. Am. Chem. Soc.* **114,** 10952 (1992).
7. T. N. Nguyen and H.-C. zur Loye, *J. Solid State Chem.* **117,** 300 (1995).
8. T. N. Nguyen, D. M. Giaquinta, and H.-C. zur Loye, *Chem. Mater.* **6,** 1642 (1994).
9. A. Furusaki, M. Sigrist, P. A. Lee, K. Tanaka, and N. Nagaosa, *Phys. Rev. Lett.* **73,** 2622 (1994).
10. T. N. Nguyen, P. A. Lee, and H.-C. zur Loye, *Science* **271,** 489 (1996).
11. C. Lampe-Önnerud and H.-C. zur Loye, *Inorg. Chem.* **35,** 2155 (1996).
12. H. McMurdie, *Powder Diff.* **1,** 76 (1986).
13. H. M. Rietveld, *J. Appl. Crystallogr.* **2,** 65 (1969).
14. A. C. Larson and R. B. Von Dreele (1994). ''General Structure Analysis System (GSAS),'' Los Alamos National Laboratory Report LAUR 86-748.
15. P. Thompson, D. E. Cox, and J. B. Hastings, *J. Appl. Crystallogr.* **20,** 79 (1987).
16. S. C. Abrahams and J. I. Bernstein, *Acta Crystallogr. B* **25,** 1233 (1969).
17. N. N. Greenwood and A. Earnshaw, ''Chemistry of the Elements.'' Pergamon Press, Oxford, 1989.
18. A. F. Cotton and G. Wilkinson, Wiley, New York, 1980.
19. A. F. Wells, ''Structural Inorganic Chemistry.'' Clarendon Press, Oxford, 1984.
20. G. V. Vajenine, R. Hoffmann, and H.-C. zur Loye, *Chem. Phys.* **204,** 469 (1996).
21. A. V. Powell, J. G. Gore, and P. D. Battle, *J. Alloys Compounds* **201,** 73 (1993).
22. R. C. Currie, J. F. Vente, E. Frikkee, and D. J. W. IJdo, *J. Solid State Chem.* **116,** 199 (1995).
23. The data in Fig. 3 are fitted by the angle averaged susceptibility of the Ising model with the Hamiltonian.

$$H = J \sum_{i=0}^{\infty} S_i^z S_{i+1}^z,$$

with J as the coupling and S_i^z the z component of the ith spin. The susceptibility is given by

$$\chi = \frac{1}{3}\chi_l + \frac{2}{3}\chi_t = \frac{Ng^2\mu_B^2}{12J}\left[Ke^{-2K} + \tanh(K) + \frac{K}{\cosh^2(K)}\right],$$

where $K = J/k_B T$, g is the gyromagnetic ratio, μ_B is the Bohr magneton, and k_B is the Boltzmann constant (24).
24. In the Ising model the angular average is taken into account, because the data were obtained from powder samples.
25. D. C. Mattis, ''The Theory of Magnetism,'' Vol. II. Springer Verlag, Berlin 1985.